BIOCHEMISTRY

Engineering a nanopore with co-chaperonin function

10.1126/sciadv.1500905

Ching-Wen Ho,[1] Veerle Van Meervelt,[1] Keng-Chang Tsai,[2] Pieter-Jan De Temmerman,[3] Jan Mast,[3] Giovanni Maglia[4]*

The emergence of an enzymatic function can reveal functional insights and allows the engineering of biological systems with enhanced properties. We engineered an alpha hemolysin nanopore to function as GroES, a protein that, in complex with GroEL, forms a two-stroke protein-folding nanomachine. The transmembrane co-chaperonin was prepared by recombination of GroES functional elements with the nanopore, suggesting that emergent functions in molecular machines can be added bottom-up by incorporating modular elements into preexisting protein scaffolds. The binding of a single-ring version of GroEL to individual GroES nanopores prompted large changes to the unitary nanopore current, most likely reflecting the allosteric transitions of the chaperonin apical domains. One of the GroEL-induced current levels showed fast fluctuations (<1 ms), a characteristic that might be instrumental for efficient substrate encapsulation or folding. In the presence of unfolded proteins, the pattern of current transitions changed, suggesting a possible mechanism in which the free energy of adenosine triphosphate binding and hydrolysis is expended only when substrate proteins are occupied.

INTRODUCTION

Engineering new functions into existing assemblies is a first step to building artificial biological systems. Biological nanopores with known structure are ideal building elements for this task because they have a robust assembly (*1*, *2*) that allows, for example, the building of protein (*3*) or protein-DNA (*4*) rotaxanes. Further, the ionic flux through a nanopore can be used to recognize molecules (*5*–*8*) or study biological and chemical processes at the single-molecule level (*8*–*11*). Although the introduction of an enzymatic function has yet to be reported, new properties have been engineered into biological nanopores. Notably, Feringa and co-workers chemically modified a mechanosensitive channel with photosensitive compounds and created a nanovalve that could open in response to light stimulus (*12*). Bayley and co-workers attached DNA (*13*) or a cyclodextrane adaptor (*14*) to an alpha hemolysin (αHL) nanopore to recognize single molecules. We recently incorporated DNA molecules atop a ClyA nanopore to build hybrid DNA-nanopore devices that were able to selectively transport DNA (*15*) or proteins (*16*) down a potential gradient across a lipid membrane. Introducing new functions encoded in the genetic sequence of the proteins, however, is more challenging (*17*), mainly because the folding of proteins is not predictable. One solution often adopted by nature is combining or swapping different evolutionarily conserved regions of proteins with generally independent structural and functional properties (domains). Here, we adopt a similar strategy and introduced the functional elements of co-chaperonin GroES into the αHL nanopore to engineer a new nanopore that monitors the GroEL reaction at the single-molecule level.

The *Escherichia coli* chaperonin GroEL and co-chaperonin GroES pair mediates the folding of many essential proteins by transducing the energy of adenosine triphosphate (ATP) binding and hydrolysis into concerted rotary motions (*18*–*23*). GroEL consists of two homo-heptameric back-to-back rings, whereas GroES is a smaller dome-shaped co-chaperonin that seals GroEL (*24*). During the GroEL reaction cycle, two major domains, an apical domain and an equatorial domain, are interconnected by a smaller intermediate domain (Fig. 1A) and undergo ATP-mediated cooperative movements (*25*, *26*) that induce the encapsulation and subsequent folding of the protein substrates within the GroEL cavity. The binding between GroEL and GroES is mediated by seven flexible loops (ES loops) that undergo folding transitions upon binding to GroEL (*24*, *27*). Because the GroEL reaction cycle ranges from 4 to 20 s depending on the temperature and the concentration of nonnative substrate protein (*18*–*23*), it is not ideally suited for monitoring with single-molecule fluorescence techniques.

Here, we show that the incorporation of the ES loops into the heptameric αHL nanopore produced a chimera protein that efficiently assisted protein folding by GroEL. These results therefore suggest that co-chaperonin function might have appeared by incorporating hydrophobic polypeptides into a preexisting protein assembly. Further, single-channel recordings allowed the investigation of the binding of GroEL to individual co-chaperonin nanopores, revealing kinetic intermediates during chaperon/co-chaperonin association.

RESULTS AND DISCUSSION

Design of a GroES nanopore

The transmembrane co-chaperonin was designed by incorporating the GroES loops into the αHL nanopore (Fig. 1, A and B, and Supplementary Discussion). Two constructs were prepared and further characterized. In the first construct, αHL-GroES$_S$, the ES loops were flanked on both sides by a serine-glycine (SG) linker (Fig. 1C). In the second construct, αHL-GroES$_L$, the ES loops were flanked by five additional residues on both sides, which come together in GroES to form a β sheet (Fig. 1, C and D). Both constructs were hemolytically active (Fig. 2A), confirming that the modifications to the nanopore structure did not compromise the folding and assembly of the nanopore.

Characterization of nanopore-GroES chimera proteins

GroEL induces the hydrolysis of ATP, whereas the binding of GroES reduces the adenosine triphosphatase (ATPase) activity by ~50% (*18*). The co-chaperonin interaction is mediated by the residues L^{234}, L^{237},

[1]Department of Chemistry, University of Leuven, Leuven 3001, Belgium. [2]National Research Institute of Chinese Medicine, Ministry of Health and Welfare, Taipei 11221, Taiwan. [3]Electron Microscopy Unit, Veterinary and Agrochemical Research Centre (CODA-CERVA), Brussels 1180, Belgium. [4]Groningen Biotechnology Institute, University of Groningen, Groningen 9747AG, Netherlands.
*Corresponding author. E-mail: g.maglia@rug.nl

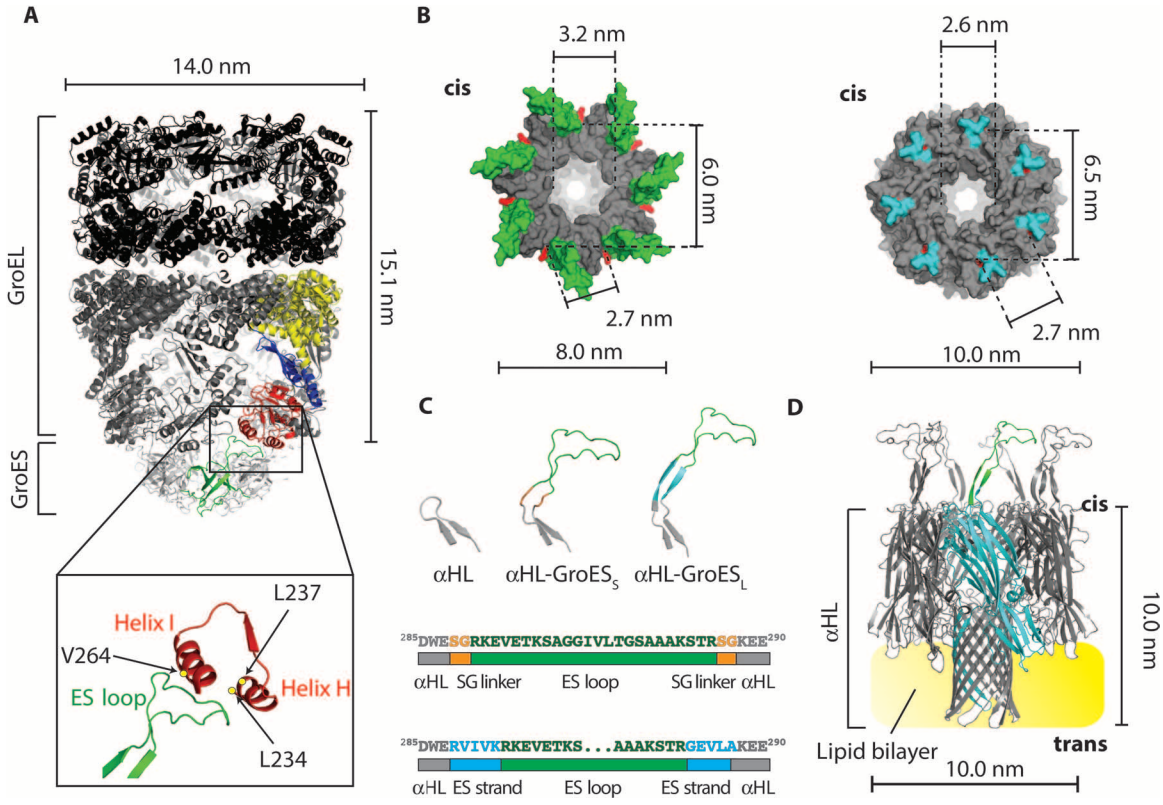

Fig. 1. A GroEL:GroES-nanopore machine. (**A**) Ribbon representation of the ADP:GroEL:GroES complex (PDB: 1AON). Single-GroES and single-GroEL subunits are colored: apical domain, red; equatorial domain, yellow; intermediate domain, blue; GroES subunit, green. The expansion shows the interaction between the ES loop and the H and I helices of the GroEL apical domain. The amino acids in GroEL that are mainly involved in the interaction with GroES (L^{234}, L^{237}, and V^{264}) are shown as yellow dots. (**B**) Surface representation of the top view of the cis side of GroES (left, PDB: 1AON) and αHL (right, PDB: 7AHL). The ES loops are green and the αHL loops are cyan. The lines indicate the diameter of the cis central apertures and the α-carbon distance of the first residue (red) of the ES loops (K^{13}) or the αHL loops (W^{286}) between adjacent and opposite subunits. (**C**) Top, β-hairpin loops in αHL (left), αHL-GroES$_S$ (center), and αHL-GroES$_L$ (right). Bottom, scheme describing ES loop insertions (green) into the αHL sequence (gray) for αHL-GroES$_S$ (top) and αHL-GroES$_L$ (bottom) constructs. The SG linker is depicted in orange and the ES strand (10 additional GroES residues that form a β strand in GroES) is shown in blue. (**D**) Ribbon representation of αHL-GroES$_L$ (gray) prepared by homology modeling from the αHL and GroES structures. An αHL subunit is shown in cyan with one ES loop in green, and the lipid bilayer is shown in yellow.

and V^{264} in GroEL (*24*), and their substitution with alanine produces a GroEL mutant (GroEL-LLV) in which ATPase activity is not inhibited by GroES (fig. S1 and table S1). We found that αHL-GroES$_S$ and αHL-GroES$_L$ decreased the ATPase activity of GroEL to 64 ± 1% (50 mM KCl, N = 10) and 58 ± 8% (50 mM KCl, N = 3), respectively, of the original activity (Fig. 2B and table S2), whereas the activity of GroEL-LLV (fig. S1 and table S1) was not changed. These results suggest, therefore, that the inhibition of wild-type GroEL activity by αHL-GroES chimeras is mostly mediated by the grafted ES loops introduced in the chimera nanopores.

We tested the ability of αHL-GroES$_S$ and αHL-GroES$_L$ in assisting GroEL in refolding malate dehydrogenase (MDH; Fig. 2C and table S3) from porcine heart and L-lactic dehydrogenase (LDH; fig. S2 and table S4). The target proteins were first unfolded in 3 M guanidinium-HCl and then diluted into a refolding buffer containing 50 nM GroEL. Refolding was initiated by the addition of 200 nM GroES or αHL variants in 2 mM ATP. Both chimera proteins were able to assist the GroEL-mediated refolding of MDH and LDH in the presence of both 50 mM KCl and 1 M KCl. Remarkably, αHL-GroES$_L$ showed the same efficiency as GroES in refolding MDH (Fig. 2C). Because αHL-GroES$_S$ was less efficient than αHL-GroES$_L$ in assisting the GroEL reaction, αHL-GroES$_L$ was used for further characterization.

The double ring of GroEL is resistant to proteolysis by proteinase K, but the last 16 C-terminal residues of each subunit are cleaved, because the proteinase is small enough to enter the GroEL cavity where the residues are lodged. The binding of GroES on top of the GroEL cylinder effectively seals the cavity of GroEL and protects the C-terminal tail from proteinase K degradation. Thus, the proteolysis of GroEL in the presence of GroES results in two bands of roughly equal intensity after analysis by SDS–polyacrylamide gel electrophoresis. As shown in Fig. 2D, αHL-GroES$_L$ was effective in protecting GroEL C termini from proteinase K digestion, indicating that αHL-GroES$_L$ is able to seal the cavity of GroEL.

As a final characterization of the interaction between GroEL and αHL-GroES$_L$, we used negative-staining transmission electron microscopy (EM) (Fig. 2E and fig. S3). Following previous studies (*25*, *26*), αHL-GroES$_L$ was incubated with a GroEL mutant containing the D398A substitution (GroEL-398) with normal ATP binding but only 2% of the wild-type ATPase activity (*28*). From 115 manually analyzed EM structures, GroEL-398:ATP:αHL-GroES$_L$ complexes displayed a mean (±SD)

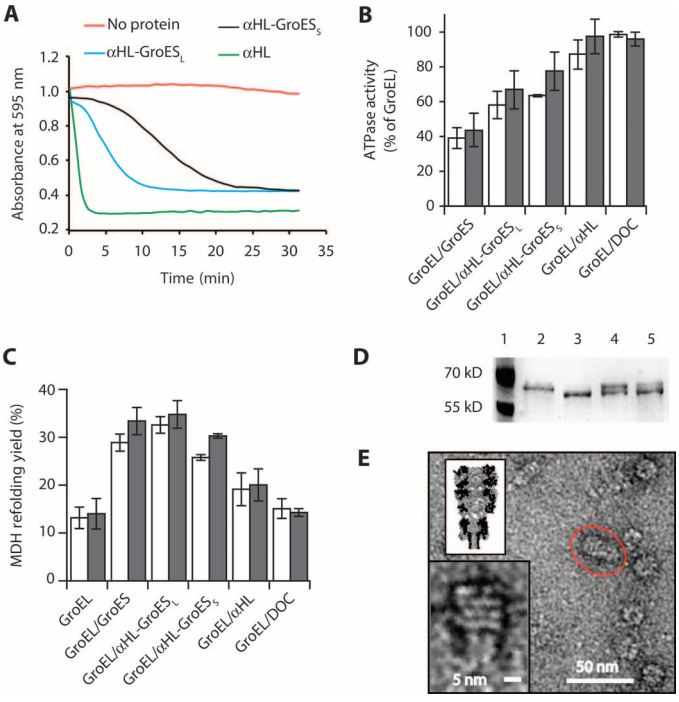

Fig. 2. Characterization of αHL-GroES chimera proteins. (**A**) Typical traces for the hemolytic assay showing the pore-forming activity of nanopore proteins. Each line shows the reduction in absorbance for monomeric nanopore proteins: αHL is in green, αHL-GroES$_L$ is in blue, and αHL-GroES$_S$ is in black. The red line shows a control experiment where no protein was used. Proteins are added to a 0.0625 μM final concentration and were incubated with a solution of diluted rabbit red blood cells in 10 mM Mops and 150 mM NaCl (pH 7.4) containing bovine serum albumin (1 mg/ml). The pore-forming activity of the αHL proteins is shown by the decrease in the absorbance at 595 nm due to the lysis of the rabbit red blood cells. (**B**) ATPase activity of GroEL (50 nM) in the presence of GroES proteins (200 nM) and/or the surfactant used to solubilize the nanopores [deoxycholate (DOC), 0.125 mM] in 50 mM KCl (white bars) or 1 M KCl (gray bars). The ATPase reaction was started by adding ATP to the reaction buffer containing GroES and GroEL proteins. The values are shown in table S2. (**C**) Refolding assay assisted by GroES proteins in 50 mM KCl (white bars) or 1 M KCl (gray bars). Unfolded MDH (2 μM) was preincubated with GroEL (50 nM) in the refolding buffer (no ATP) before the addition of ATP (2 mM) and co-chaperonin proteins (200 nM). Control experiments with DOC and αHL indicated that the GroEL-assisted refolding is mediated by the grafted loops in αHL-GroES$_L$. Refolding yields were normalized by the spontaneous refolding of MDH. The values are shown in table S3. (**D**) Proteinase K protection assay. GroEL (0.2 μM), preincubated with GroES or αHL-GroES$_L$ (1 μM) in lanes 4 and 5, respectively, was treated with proteinase K (25 μg/ml) in the presence of ATP (1 mM) for 20 min before loading into polyacrylamide SDS gels. Lane 1, protein ladder. Lane 2, undigested GroEL (58 kD). Lane 3, GroEL after incubation with proteinase K (~56 kD). Lane 4, GroEL digestion protected by GroES. Lane 5, GroEL digestion protected by αHL-GroES$_L$. (**E**) Negative-stained EM image of GroEL-398 bound to αHL-GroES$_L$ formed by preincubating GroEL-398 (0.5 μM) with αHL-GroES$_L$ (1 μM) for 20 min before applying a 100-fold dilution to negatively stained EM grids. The insets show the magnification of the circled complex (bottom) and a scaled surface representation of the αHL-GroES$_L$:GroEL complex (top). Experiments and dilutions in (B) and (C) were carried out in 50 mM tris-HCl (pH 7.5), 50 mM KCl, 1 mM ATP, and 5 mM $MgCl_2$. Errors are quoted as SD.

length of 254 ± 35 Å. In agreement with GroEL adopting a "bullet" configuration (*24*) (Fig. 1A and fig. S3), the width of the complexes measured 145 ± 20 Å at the GroEL end and 100 ± 19 Å at the equatorial position where GroEL interacted with αHL-GroES$_L$.

Single-channel recordings with a single-ring GroEL

To investigate the intermediates of the chaperonin–co-chaperonin interaction and the folding of proteins inside the chaperonin cavity by single-channel recordings, we used a single-ring variant of GroEL (SR1), where the amino acids that mediate the contacts between the two rings were replaced by alanine or glutamic acid (*29*). SR1 binds normally to GroES and resembles the folding-active state of GroEL. However, because it lacks the trans ring, SR1 produces only one refolding cycle, providing an ideal system to study the chaperonin–co-chaperonin protein folding reaction without the complication of off-path reactions in the trans ring.

At +100 mV, the open pore current of individual αHL-GroES$_L$ nanopores (I_O = 109.3 ± 4.4 pA, n = 10) was similar to that of wild-type αHL (*30*), suggesting that the ES loops did not occlude the αHL nanopore. The addition of SR1 to the cis compartment of αHL-GroES$_L$ in the presence of ATP produced long-lasting current blockades (Fig. 3A). Fifty percent of the blockades released spontaneously with an average dwell time (τ) of 55 ± 5 s (N = 8, n = 134). In the remaining 50% of observed events, GroEL did not release from αHL-GroES$_L$, and the open pore current could only be obtained by ramping the applied potential to −100 mV (Fig. 3A). Similar current blockades were observed when SR1 was used with the nonhydrolyzable ATP analog adenylyl-imidodiphosphate (AMP-PNP), although the blockades were always transient (τ = 157 ± 64 s, N = 6, n = 50; Fig. 3B). In the absence of nucleotides (fig. S4) or in the presence of ADP (Fig. 3C), these long blockades were not observed, indicating that ATP mediates the interaction of SR1 with the GroES rings.

GroEL intermediate states

Among the current blockades, six different types of current signatures were identified: L1, L2, L3, S4, S5, and L6 (Figs. 3A and 4A), in which the prefix "L" indicates a well-defined current level and the prefix "S" indicates a current state characterized by multiple transitions among different current levels. All current levels were observed when AMP-PNP was used instead of ATP (Fig. 3, A and B), suggesting that they reflected ATP-bound configurations. The current blockades proceeded in successive steps with no backward transitions. Among the blockades recorded, 6% started with L1, 77% with L2, 15% with L3, and 1% with L6 (N = 8, n = 134). L1 current levels (I_B, ~20 pA) were very short (<1 ms), and the dwell time (τ) could not be accurately measured. L2 and L3 current levels showed a blocked current level (I_B) of 2.1 ± 0.2 and 10.1 ± 0.5 pA, respectively, and a dwell time of 8.4 ± 0.4 and 10.3 ± 0.6 ms, respectively (Fig. 4A). The subsequent current state S4 (τ = 55 ± 5 s) was characterized by a dominant current level (L4a, 5.2 ± 0.2 pA) that regularly visited a second level (L4b, ~20 pA; fig. S5).

The S4 current transition resulted in the release of the complex in 50% of events (fig. S6A), whereas S4 switched to an L6 level in the remaining 50% of the observed events (12.0 ± 0.5 pA, N = 10, n = 38; Fig. 4A and fig. S6A). Both transitions were preceded by S5, a fast current state (τ = 18.0 ± 0.3 ms) with undefined current levels (average I_B, ~10 pA; Fig. 4A and fig. S6A). At positive potentials, L6 lasted indefinitely, indicating that the SR1:ATP:αHL-GroES$_L$ ternary complex did not spontaneously dissociate. The release of GroES from the ADP:GroEL:GroES complex is induced by intraring conformational

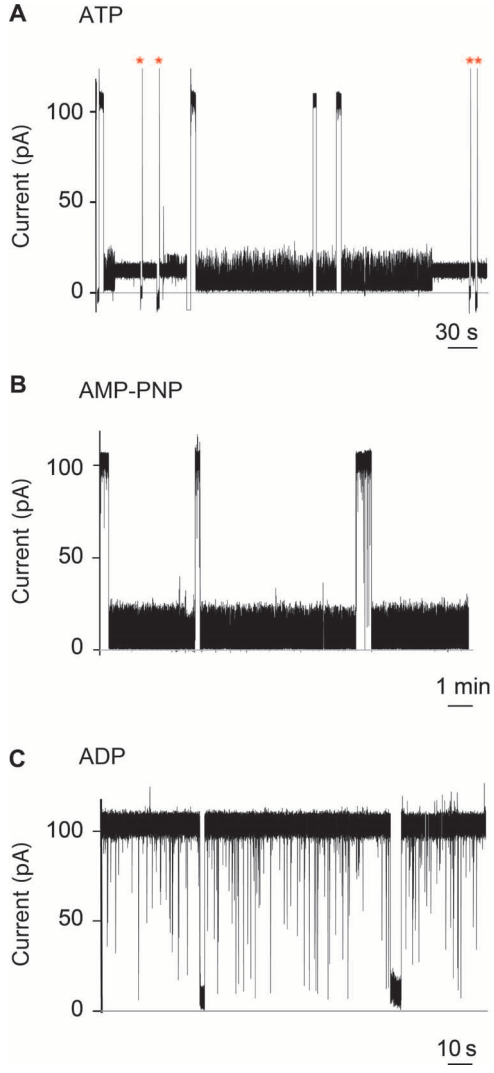

Fig. 3. Interaction of SR1 with membrane-bound αHL-GroES$_L$ monitored by single-molecule recordings. (**A** to **C**) Current blockades provoked by SR1 to αHL-GroES$_L$ in the presence of 1 mM ATP (A), the nonhydrolyzable ATP analog AMP-PNP (B), or adenosine diphosphate (ADP) (C) added to the cis chamber at +100 mV. The current blockades are due to the interaction of the chaperonin with individual engineered co-chaperonin nanopores. (A) Fifty percent of the blockades in the presence of ATP were transient (dwell time, 55 ± 5 s; main I_B value, 5.2 ± 0.2 pA), showing fast current fluctuations (see the text and fig. S5). The remaining current blockades switched to a quieter and permanent current level (I_B value, 12.5 ± 0.5 pA). The open pore current could only be obtained by multiple ramping of the potential to +100/−100 mV (red asterisks). (B) AMP-PNP–induced current blockades showed the same current level as ATP-induced blockades but were always transient (average dwell time, 157 ± 64 s; main I_B value, 5.2 ± 0.1 pA) (see the text). (C) In the presence of ADP, the current blockades were transient, showing a dwell time faster than the resolution of our current recordings (dwell time, <1 ms). Occasionally longer current blockades were observed, which showed an I_B value of 3.0 ± 1.4 pA (fig. S6c). The electrical recordings were carried out in 1 M KCl, 50 mM tris-HCl (pH 7.5), and 5 mM $MgCl_2$ at 23°C and +100 mV by applying a 10-kHz low-pass Bessel filter with a 50-kHz sampling rate. An additional digital Gaussian filter at 2 kHz was applied to current traces.

changes that follow the cooperative binding of ATP to the opposite ring (*20*, *21*, *28*, *29*, *31*–*33*), and the absence of intraring contact in the single-ring version SR1 produces a chaperonin that cannot release from GroES (*29*). In the presence of AMP-PNP, S5 was slower (τ = 195 ± 17 ms) and an intermediate current level was observed (L5, 7.9 ± 1.8 pA, N = 5, n = 49; fig. S6B). Fifty-seven percent of the L6 ternary AMP-PNP:SR1:αHL-GroES$_L$ complexes released spontaneously in less than 2 min, indicating that the AMP-PNP complex was less stable than the respective ATP complex.

Many structural studies showed that GroEL cycles between several intermediate structures characterized by large conformational changes of the chaperonin apical domains (*34*). Therefore, it is likely that changes in the ionic current through αHL-GroES$_L$ nanopores reflected the cycling of GroEL through several conformational changes. Although a precise assignment of the current levels described by SR1 docking to αHL-GroES$_L$ to intermediate states in the chaperonin can only be speculative, L1, L2, L3, and S4 current blockades might correspond to four prehydrolytic GroEL structures previously observed using stopped-flow experiments with an engineered single-tryptophan variant of GroEL and SR1 (*35*, *36*). S4 showed fast current transitions (<1 ms), suggesting a dynamic ATP-bound GroEL structure. Fast conformational transitions associated to the binding of ATP to GroEL (<10 ms) have been observed using fluorescence (*35*, *37*) and single-molecule atomic force microscopy (*38*) studies. A dynamic S4 might then correspond to the ATP:R-ES (*25*, *39*) or ADP:GroEL$_{D83A/R197A}$ structure (*40*), which shows a relaxed nucleotide-bound state where the interapical salt bridges are broken and the apical domains adopt highly dynamic and asymmetric configurations. The flexibility of the apical domains could be an important feature in GroEL catalysis that might allow the interaction of GroEL with diverse substrate proteins (*40*, *41*). The absence of the cis ring allows the SR1 to adopt an expanded conformation not accessible to GroEL and observed in a cryo-EM study [SR1^{D398A}:ATP:GroES (*34*)]. This configuration could correspond to the L6 current level.

Possible mechanism for GroEL-induced current blockades

In nanopore recordings, molecules are usually recognized as they bind to the interior of the pore (lumen), where the potential drop and the resistance to the ionic flow are high (*42*, *43*). Proteins binding to the cis side of αHL either induce small current blockades (*44*) or, most often, are not observed, as shown by many previous studies with proteins holding or controlling the motion of individual DNA molecules threading the nanopore (*11*, *45*–*49*). Therefore, it is surprising that the binding of GroEL to αHL-GroES$_L$, which takes place outside the lumen of the nanopore, produced the large current blockades observed in this work. A possible explanation is that the binding of GroEL to αHL-GroES$_L$ produces a tight seal at the nanopore entrance. However, this is unlikely because the GroES loops grafted at the top of αHL included relatively long linkers (Fig. 1). In addition, GroEL has a hollow cylindrical surface that is expected to provide little resistance to the ionic flow. Another possibility is that the twists and turns of GroEL apical domains induced a conformational change throughout the αHL nanopore that, like the iris of a camera, reduced the size of the nanopore.

Monitoring the SR1-assisted protein refolding with αHL-GroES$_L$ nanopores

Next, we investigated the refolding of protein substrates (DHFR, MDH, or rhodanese) with SR1. SR1-substrate complexes were formed by rapidly mixing urea-denatured protein substrates (DHFR, MDH, or

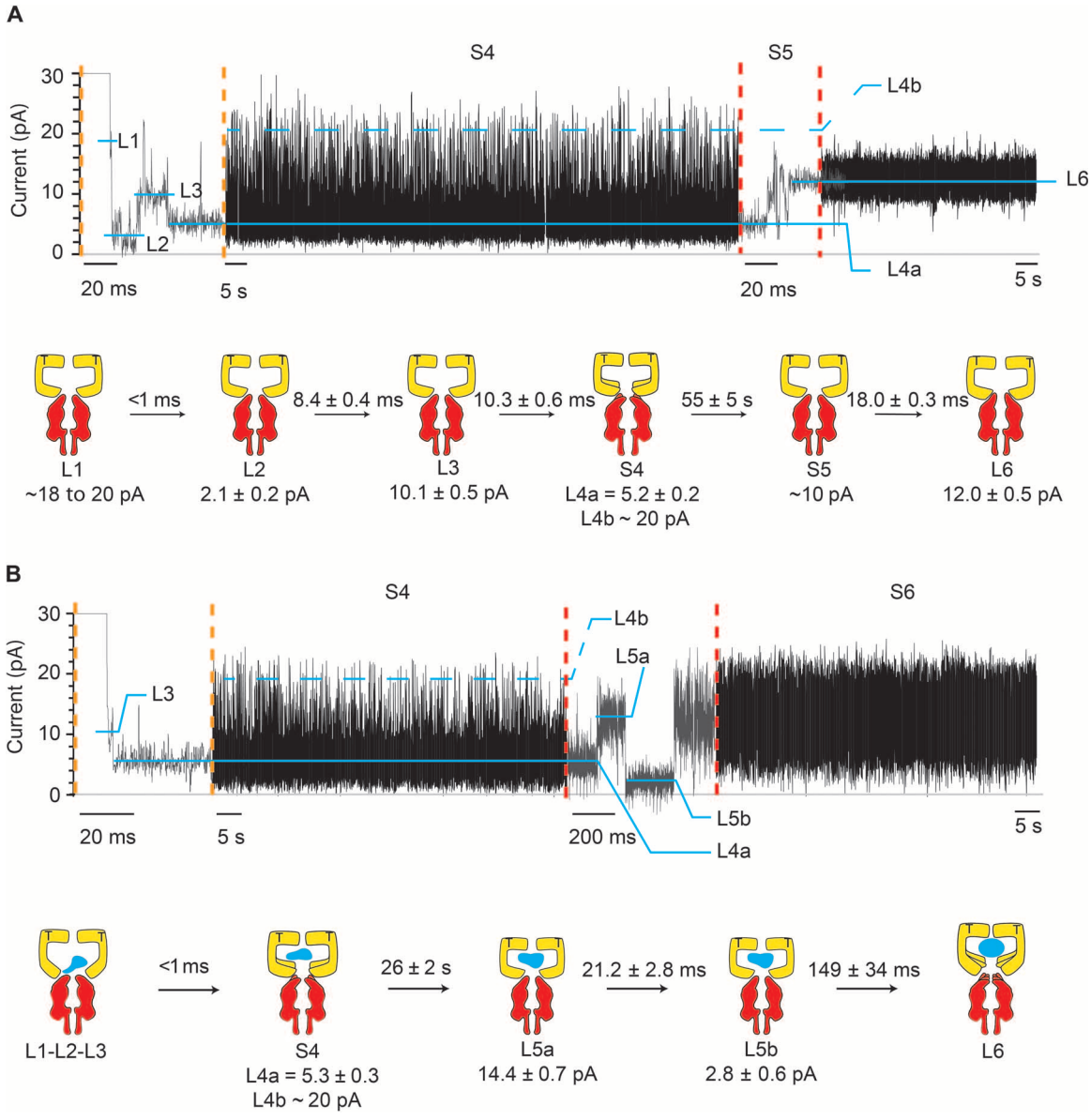

Fig. 4. Intermediates of SR1 protein-folding cycle. Typical SR1 current blockades. The current traces between the vertical dotted orange and red lines are expansions of the main current traces showing the fast current transitions that characterize the L1, L2, L3, and S5 states. The cartoon depictions below the current traces show the kinetic succession between SR1 intermediates. SR1 is in yellow, αHL-GroES$_L$ is in red, and the substrate protein is in blue. (**A**) αHL-GroES$_L$ current blockade for the ternary SR1:ATP:αHL-GroES$_L$ complex. L1 (dwell time, <1 ms) was observed only in a few blockades (6%). Ninety-two percent of blockades started with either L2 (77%) or L3 (15%) current levels. The transition from S4 to L6 was fast (10.3 ± 0.6 ms; fig. S5) and characterized by current fluctuations showing an average value at ~10 pA. An expansion of the S4 current state is shown in fig. S5. (**B**) αHL-GroES$_L$ current blockade for the quaternary SR1:ATP:DHFR:αHL-GroES$_L$ complex. In 91% of blockades, L1, L2, and L3 current levels could not be sampled, whereas the transition between S4 and L6 showed two well-defined current levels, indicating that the unfolded protein modified the interaction of SR1 with αHL-GroES$_L$ (see the text). Dihydrofolate reductase (DHFR) was urea unfolded and incubated with SR1 before addition to the cis chamber. Traces were recorded in 1 M KCl and 50 mM tris-HCl (pH 7.5) at 23°C in the presence of 1 mM ATP and 5 mM $MgCl_2$ by applying a 10-kHz low-pass Bessel filter and using a 20-μs (50-kHz) sampling rate. An additional postacquisition Gaussian filter at 2 kHz was then applied to the current traces.

rhodanese) with SR1 and then added to the cis side of an individual αHL-GroES$_L$ nanopore in the presence of 1 mM ATP. Under these conditions, L1 was no longer observed (n = 271, N = 9), whereas only 9% of the blockades started with L2 that rapidly turned into L3 and then an S4 blockade. The remaining blockades started either with S4 (62%) or with a new current state S6 (29%; fig. S7). S6 blockades, which often followed S4 and most likely corresponded to L6 levels in the ATP:SR1:αHL-GroES$_L$ complex, showed a plethora of different current signatures (Fig. 4B and fig. S7) that mostly fluctuated between ~15- and ~20-pA current levels. The S4 dwell time for the ATP:SR1:substrate:αHL-GroES$_L$ (quaternary) complexes was about 2-fold shorter than that for the ATP:SR1:αHL-GroES$_L$ (ternary) complex, whereas the S5 current

transition was ~10-fold longer (Fig. 4). Finally, in several collected events for the quaternary complex (n = 45, N = 10), the ionic current of S6 dropped to a new current level, L7 (I_B, 4.3 ± 0.9 pA; τ = 60 ± 29 ms; fig. S7), in less than 2 min before returning to the open pore current. Because L7 resembled the ADP-bound state of SR1 (Fig. 3C and fig. S6), these results suggest that the presence of unfolded protein inside the SR1 cavity might induce the nucleotide hydrolytic active GroEL configuration and promote the release of SR1.

Role of GroEL intermediates during chaperonin-mediated protein folding

These results might shed light on a conundrum in the GroEL reaction cycle, that is, how the competitive displacement of substrates by GroES during encapsulation could promote the ejection of substrate proteins from the binding site into the folding chamber with no release of the substrate into solution. One previously suggested possibility was that substrate proteins bind first and the arrival of ATP induces conformational changes that induce a forced unfolding of the substrate protein and position the protein for efficient encapsulation (*26*, *50*). However, it was observed that in the presence of both ATP and unfolded proteins, the nucleotides bind first (*36*, *51*), suggesting that the ATP-induced movement might actually precede the binding of substrate proteins.

Here, we show that in complexes with substrate proteins, most of the SR1:ATP molecules bound to αHL-GroES$_L$ begin with L3 or S4, which corresponded to a "late" structural intermediate. By contrast, in the absence of substrate proteins, SR1:ATP interacted with the ES loops of αHL-GroES$_L$ mainly with an L1 or L2 state, corresponding to an "early" structural intermediate. Therefore, the binding of ATP to the SR1-substrate complex induced the apical domain movements before the interaction with the ES loops. By contrast, the binding of ATP to apoSR1 induced only the initial apical domain movements in SR1, and only the docking to the hydrophobic GroES loops induced the folding-active and dynamic S4 state (Fig. 4). Therefore, our results suggest that the order of ATP arrival is irrelevant to obtaining the active folding GroEL structure, because the cooperative rigid-body rotations of the apical domain that position the substrate protein for optimal internalization only happen if both ATP and the substrate protein are bound to GroEL. The subsequent contact with GroES would then displace the hydrophobic residues in the substrate protein, releasing the polypeptide substrate into the hydrophilic folding chamber in which the polypeptide can fold in solitude.

CONCLUSIONS

We constructed a nanopore with enzymatic activity by fusing the flexible loops of GroES with a biological nanopore. Remarkably, the transmembrane GroES nanopore mediated GroEL-assisted protein folding as efficiently as native GroES, indicating that the only functional elements of GroES are its flexible loops. The mechanism by which new functions are added to molecular machines remains an unanswered question (*52*). Here, we showed that co-chaperonin functionality can be introduced bottom-up by adding modular elements into an unrelated globular structure, suggesting a possible path during GroEL-GroES evolution in which the co-chaperonin function appeared sequentially by incorporating hydrophobic polypeptide loops into preexisting protein assemblies.

Single-channel experiments with the SR1-nanopore chimera combined high-sampling rates with long observation times and allowed the examination of details not easily accessible with other biophysical techniques. Similar approaches might be used to engineer αHL or other nanopores to study proteins with a toroid shape (for example, ClpX or AAA ATPase proteins). Here, we showed that the modulation of the ionic current through the GroES nanopore revealed that the GroEL catalytic cycle might include at least four co-chaperonin and ATP-bound intermediate states. One such state is highly dynamic, showing fluctuations of less than 1 ms, a characteristic that could be instrumental for efficient substrate encapsulation. Finally, we observed that in the presence of unfolded substrate proteins, the pattern of the chaperonin current blockades was changed. Our results suggest that the movement of the apical domains of GroEL is activated only when the binding sites of both substrate proteins and ATP are occupied.

MATERIALS AND METHODS

Detailed methods are available in the Supplementary Materials.

Materials

Chemicals were purchased from Sigma and enzymes were obtained from Fermentas, if not otherwise specified. Lipids were purchased from Avanti Polar Lipids and DNA was acquired from Integrated DNA Technologies. The genes encoding for αHL-GroESS, GroEL, and GroES were constructed by GenScript.

Protein preparation

Constructs were prepared using the MEGAWHOP procedure (*53*, *54*) or by site-directed mutagenesis (Stratagene). GroEL, GroEL-LVV, and GroEL-398 (*55*–*57*); αHL, αHL-GroES$_S$, and αHL-GroES$_L$ (*58*, *59*); and GroES were purified following previously described protocols. MDH, rhodanese, and LDH were purchased from Sigma. A detailed description of protein preparation is available in the Supplementary Materials.

Protein assays

GroEL ATPase assays (*60*), MDH (*61*) and LDH (*62*) refolding assays, and the proteinase K protection assay (*17*) were performed following previously described protocols. A detailed description of such assays is available in the Supplementary Materials.

Electrical recordings from planar lipid bilayers

Single-channel recordings were performed using 1,2-diphytanoyl-*sn*-glycero-3-phosphocholine (Avanti Polar Lipids) bilayers dividing two chambers, each containing 500 μl of buffer as described in detail by Maglia *et al.* (*63*). The electrical signals were amplified by using an Axopatch 200B patch clamp amplifier (Axon Instruments) with the cis compartment connected to ground. Amplified signals were digitized with a Digidata 1320 A/D converter (Axon Instruments) using Clampex 10.2 software (Molecular Devices). Data analysis was carried out using Clampfit (Molecular Devices). In single-channel recordings, after the reconstitution of individual conductive channels, the protein excess was removed by perfusion of the cis solution.

Data analysis

Individual dwell times were collected manually using Clampfit 10.2 software (Molecular Devices). Values were then binned to create a

histogram and fitted to single-exponential functions (standard exponential, Clampfit). The mean lifetimes corresponded to the average dwell times quoted in the manuscript, and the errors were the SEs of the fits. Blocked current values were calculated from Gaussian fit to all-point histograms. The values were then averaged and the errors were given as SDs.

Homology model of GroEL:αHL-GroES$_L$

The mobile loops of the seven GroES subunits (from Arg^9 to Ala^{42}) were manually grafted to Glu^{288} and Lys^{289} on the loop of αHL (loop C sequence, YKIDWE288K289EEMTN) to produce the initial structure. The initial structure including the target sequence was then refined by homology modeling to establish a reliable and complete αHL-mobile loop model. The homology model of αHL-GroES$_L$ was generated by the MODELER v.9.4 program in Discovery Studio v.3.5 (Accelrys Software Inc.) using the crystallographic structures of the GroES mobile loop [Protein Data Bank (PDB): 1AON] and that of αHL (PDB: 7AHL) as structural templates. The homology model of αHL-GroES$_L$ was energy-minimized at the linkage of the insert by using a Dreiding-like force field for a few steps to remove any bad contacts.

Sample preparation and negative-stain EM grid preparation

GroEL-398 (0.5 μM) and αHL-GroES$_L$ (1 μM) were added to a solution containing ATP (2 mM), tris-HCl (50 mM; pH 7.5), KCl (50 mM), and $MgCl_2$ (5 mM) and then incubated at 25°C for 20 min to allow the formation of the protein complex. A 100-fold diluted mixture in the same buffer was then applied to pioloform- and carbon-coated 400-mesh copper grids (Agar Scientific). These grids were glow-discharged for 30 s at 0.38 mbar and 15 mA (PELCO easiGlow, Ted Pella Inc.) to increase hydrophilicity. The grids were deposited on a 15-μl drop of solution for 10 min and rinsed two times with ddH_2O. Afterward, the grids were stained for 10 s with a drop of 2% uranyl acetate (Agar Scientific), blotted, and air-dried.

EM and two-dimensional image analysis

The samples were imaged in bright-field mode using a Tecnai Spirit TEM (FEI) with Biotwin lens configuration operating at 120 kV. Micrographs were recorded using a 4 × 4 K charge-coupled device camera (Eagle, FEI) at magnifications ranging from ×23,000 to ×68,000 with a corresponding pixel size of 4.9 and 1.6 Å. The pore complexes were measured manually using the "arbitrary line tool" of the iTEM image analysis software (Olympus).

SUPPLEMENTARY MATERIALS

Supplementary material for this article is available at http://advances.sciencemag.org/cgi/content/full/1/11/e1500905/DC1

Discussion

Design of the transmembrane co-chaperonin

Voltage dependence of the GroEL:αHL-GroES$_L$ interaction

Additional experimental and procedures

Fig. S1. GroEL-LLV ATPase activity.

Fig. S2. LDH refolding assay.

Fig. S3. Representative EM micrograph of single αHL-GroES$_L$:GroEL complexes.

Fig. S4. Nucleotide dependency of SR1 interaction with αHL-GroES$_L$.

Fig. S5. Expansions of an SR1-induced current blocked.

Fig. S6. Release of the binary SR1 current.

Fig. S7. Ternary SR1 current blockades.

Table S1. Percentage of GroEL-LLV ATPase activity in the presence of GroES or αHL constructs.

Table S2. Percentage of GroEL ATPase activity in the presence of GroES, αHL constructs, and/or DOC.

Table S3. MDH refolding yield catalyzed by GroEL in the presence and absence of GroES, αHL constructs, and/or DOC.

Table S4. LDH refolding yield catalyzed by GroEL in the presence and absence of GroES, αHL constructs, and/or DOC.

REFERENCES AND NOTES

1. G. Maglia, M. Henricus, R. Wyss, Q. Li, S. Cheley, H. Bayley, DNA strands from denatured duplexes are translocated through engineered protein nanopores at alkaline pH. *Nano Lett.* **9**, 3831–3836 (2009).
2. D. Japrung, M. Henricus, Q. Li, G. Maglia, H. Bayley, Urea facilitates the translocation of single-stranded DNA and RNA through the α-hemolysin nanopore. *Biophys. J.* **98**, 1856–1863 (2010).
3. A. Biesemans, M. Soskine, G. Maglia, A protein rotaxane controls the translocation of proteins across a ClyA nanopore. *Nano Lett.* **15**, 6076–6081 (2015).
4. J. Sánchez-Quesada, A. Saghatelian, S. Cheley, H. Bayley, M. R. Ghadiri, Single DNA rotaxanes of a transmembrane pore protein. *Angew. Chem. Int. Ed.* **43**, 3063–3067 (2004).
5. S. M. Bezrukov, I. Vodyanoy, V. A. Parsegian, Counting polymers moving through a single ion channel. *Nature* **370**, 279–281 (1994).
6. J. J. Kasianowicz, E. Brandin, D. Branton, D. W. Deamer, Characterization of individual polynucleotide molecules using a membrane channel. *Proc. Natl. Acad. Sci. U.S.A.* **93**, 13770–13773 (1996).
7. L.-Q. Gu, O. Braha, S. Conlan, S. Cheley, H. Bayley, Stochastic sensing of organic analytes by a pore-forming protein containing a molecular adapter. *Nature* **398**, 686–690 (1999).
8. V. Van Meervelt, M. Soskine, G. Maglia, Detection of two isomeric binding configurations in a protein-aptamer complex with a biological nanopore. *ACS Nano* **8**, 12826–12835 (2014).
9. T. Luchian, S.-H. Shin, H. Bayley, Kinetics of a three-step reaction observed at the single-molecule level. *Angew. Chem. Int. Ed.* **42**, 1926–1929 (2003).
10. M. Soskine, A. Biesemans, G. Maglia, Single-molecule analyte recognition with ClyA nanopores equipped with internal protein adaptors. *J. Am. Chem. Soc.* **137**, 5793–5797 (2015).
11. L. Franceschini, E. Mikhailova, H. Bayley, G. Maglia, Nucleobase recognition at alkaline pH and apparent pK_a of single DNA bases immobilised within a biological nanopore. *Chem. Commun.* **48**, 1520–1522 (2012).
12. A. Koçer, M. Walko, W. Meijberg, B. L. Feringa, A light-actuated nanovalve derived from a channel protein. *Science* **309**, 755–758 (2005).
13. S. Howorka, S. Cheley, H. Bayley, Sequence-specific detection of individual DNA strands using engineered nanopores. *Nat. Biotechnol.* **19**, 636–639 (2001).
14. H.-C. Wu, Y. Astier, G. Maglia, E. Mikhailova, H. Bayley, Protein nanopores with covalently attached molecular adapters. *J. Am. Chem. Soc.* **129**, 16142–16148 (2007).
15. L. Franceschini, M. Soskine, A. Biesemans, G. Maglia, A nanopore machine promotes the vectorial transport of DNA across membranes. *Nat. Commun.* **4**, 2415 (2013).
16. M. Soskine, A. Biesemans, B. Moeyaert, S. Cheley, H. Bayley, G. Maglia, An engineered ClyA nanopore detects folded target proteins by selective external association and pore entry. *Nano Lett.* **12**, 4895–4900 (2012).
17. M. Soskine, A. Biesemans, M. De Maeyer, G. Maglia, Tuning the size and properties of ClyA nanopores assisted by directed evolution. *J. Am. Chem. Soc.* **135**, 13456–13463 (2013).
18. J. Martin, M. Mayhew, T. Langer, U. Hartl, The reaction cycle of GroEL and GroES in chaperonin-assisted protein folding. *Nature* **366**, 228–233 (1993).
19. S. G. Burston, N. A. Ranson, A. R. Clarke, The origins and consequences of asymmetry in the chaperonin reaction cycle. *J. Mol. Biol.* **249**, 138–152 (1995).
20. H. S. Rye, A. M. Roseman, S. Chen, K. Furtak, W. A. Fenton, H. R. Saibil, A. L. Horwich, GroEL-GroES cycling: ATP and nonnative polypeptide direct alternation of folding-active rings. *Cell* **97**, 325–338 (1999).
21. J. P. Grason, J. S. Gresham, G. H. Lorimer, Setting the chaperonin timer: A two-stroke, two-speed, protein machine. *Proc. Natl. Acad. Sci. U.S.A.* **105**, 17339–17344 (2008).
22. F. U. Hartl, M. Hayer-Hartl, Converging concepts of protein folding in vitro and in vivo. *Nat. Struct. Mol. Biol.* **16**, 574–581 (2009).
23. H. R. Saibil, W. A. Fenton, D. K. Clare, A. L. Horwich, Structure and allostery of the chaperonin GroEL. *J. Mol. Biol.* **425**, 1476–1487 (2013).
24. Z. Xu, A. L. Horwich, P. B. Sigler, The crystal structure of the asymmetric GroEL–GroES–$(ADP)_7$ chaperonin complex. *Nature* **388**, 741–750 (1997).
25. D. K. Clare, D. Vasishtan, S. Stagg, J. Quispe, G. W. Farr, M. Topf, A. L. Horwich, H. R. Saibil, ATP-triggered conformational changes delineate substrate-binding and -folding mechanics of the GroEL chaperonin. *Cell* **149**, 113–123 (2012).
26. D.-H. Chen, D. Madan, J. Weaver, Z. Lin, G. F. Schröder, W. Chiu, H. S. Rye, Visualizing GroEL/ES in the act of encapsulating a folding protein. *Cell* **153**, 1354–1365 (2013).
27. S. J. Landry, J. Zeilstra-Ryalls, O. Fayet, C. Georgopoulos, L. M. Gierasch, Characterization of a functionally important mobile domain of GroES. *Nature* **364**, 255–258 (1993).
28. H. S. Rye, S. G. Burston, W. A. Fenton, J. M. Beechem, Z. Xu, P. B. Sigler, A. L. Horwich, Distinct actions of *cis* and *trans* ATP within the double ring of the chaperonin GroEL. *Nature* **388**, 792–798 (1997).

29. J. S. Weissman, C. M. Hohl, O. Kovalenko, Y. Kashi, S. Chen, K. Braig, H. R. Saibil, W. A. Fenton, A. L. Horwich, Mechanism of GroEL action: Productive release of polypeptide from a sequestered position under GroES. *Cell* **83**, 577–587 (1995).
30. G. Maglia, M. R. Restrepo, E. Mikhailova, H. Bayley, Enhanced translocation of single DNA molecules through α-hemolysin nanopores by manipulation of internal charge. *Proc. Natl. Acad. Sci. U.S.A.* **105**, 19720–19725 (2008).
31. N. M. Kad, N. A. Ranson, M. J. Cliff, A. R. Clarke, Asymmetry, commitment and inhibition in the GroE ATPase cycle impose alternating functions on the two GroEL rings. *J. Mol. Biol.* **278**, 267–278 (1998).
32. J. Ma, M. Karplus, The allosteric mechanism of the chaperonin GroEL: A dynamic analysis. *Proc. Natl. Acad. Sci. U.S.A.* **95**, 8502–8507 (1998).
33. M. J. Cliff, N. M. Kad, N. Hay, P. A. Lund, M. R. Webb, S. G. Burston, A. R. Clarke, A kinetic analysis of the nucleotide-induced allosteric transitions of GroEL. *J. Mol. Biol.* **293**, 667–684 (1999).
34. D.-H. Chen, J.-L. Song, D. T. Chuang, W. Chiu, S. J. Ludtke, An expanded conformation of single-ring GroEL-GroES complex encapsulates an 86 kDa substrate. *Structure* **14**, 1711–1722 (2006).
35. M. Taniguchi, T. Yoshimi, K. Hongo, T. Mizobata, Y. Kawata, Stopped-flow fluorescence analysis of the conformational changes in the GroEL apical domain: Relationships between movements in the apical domain and the quaternary structure of GroEL. *J. Biol. Chem.* **279**, 16368–16376 (2004).
36. M. J. Cliff, C. Limpkin, A. Cameron, S. G. Burston, A. R. Clarke, Elucidation of steps in the capture of a protein substrate for efficient encapsulation by GroE. *J. Biol. Chem.* **281**, 21266–21275 (2006).
37. D. Poso, A. R. Clarke, S. G. Burston, Identification of a major inter-ring coupling step in the GroEL reaction cycle. *J. Biol. Chem.* **279**, 38111–38117 (2004).
38. M. Yokokawa, C. Wada, T. Ando, N. Sakai, A. Yagi, S. H. Yoshimura, K. Takeyasu, Fast-scanning atomic force microscopy reveals the ATP/ADP-dependent conformational changes of GroEL. *EMBO J.* **25**, 4567–4576 (2006).
39. C. Chaudhry, A. L. Horwich, A. T. Brunger, P. D. Adams, Exploring the structural dynamics of the *E. coli* chaperonin GroEL using translation-libration-screw crystallographic refinement of intermediate states. *J. Mol. Biol.* **342**, 229–245 (2004).
40. X. Fei, D. Yang, N. LaRonde-LeBlanc, G. H. Lorimer, Crystal structure of a GroEL-ADP complex in the relaxed allosteric state at 2.7 Å resolution. *Proc. Natl. Acad. Sci. U.S.A.* **110**, E2958–E2966 (2013).
41. A. Horovitz, K. R. Willison, Allosteric regulation of chaperonins. *Curr. Opin. Struct. Biol.* **15**, 646–651 (2005).
42. A. Aksimentiev, K. Schulten, Imaging α-hemolysin with molecular dynamics: Ionic conductance, osmotic permeability, and the electrostatic potential map. *Biophys. J.* **88**, 3745–3761 (2005).
43. S. Howorka, H. Bayley, Probing distance and electrical potential within a protein pore with tethered DNA. *Biophys. J.* **83**, 3202–3210 (2002).
44. D. Rotem, L. Jayasinghe, M. Salichou, H. Bayley, Protein detection by nanopores equipped with aptamers. *J. Am. Chem. Soc.* **134**, 2781–2787 (2012).
45. B. Hornblower, A. Coombs, R. D. Whitaker, A. Kolomeisky, S. J. Picone, A. Meller, M. Akeson, Single-molecule analysis of DNA-protein complexes using nanopores. *Nat. Methods.* **4**, 315–317 (2007).
46. S. L. Cockroft, J. Chu, M. Amorin, M. R. Ghadiri, A single-molecule nanopore device detects DNA polymerase activity with single-nucleotide resolution. *J. Am. Chem. Soc.* **130**, 818–820 (2008).
47. D. Stoddart, A. J. Heron, E. Mikhailova, G. Maglia, H. Bayley, Single nucleotide discrimination in immobilized DNA oligonucleotides with a biological nanopore. *Proc. Natl. Acad. Sci. U.S.A.* **106**, 7702–7707 (2009).
48. F. Olasagasti, K. R. Lieberman, S. Benner, G. M. Cherf, J. M. Dahl, D. W. Deamer, M. Akeson, Replication of individual DNA molecules under electronic control using a protein nanopore. *Nat. Nanotechnol.* **5**, 798–806 (2010).
49. K. R. Lieberman, G. M. Cherf, M. J. Doody, F. Olasagasti, Y. Kolodji, M. Akeson, Processive replication of single DNA molecules in a nanopore catalyzed by phi29 DNA polymerase. *J. Am. Chem. Soc.* **132**, 17961–17972 (2010).
50. Z. Lin, D. Madan, H. S. Rye, GroEL stimulates protein folding through forced unfolding. *Nat. Struct. Mol. Biol.* **15**, 303–311 (2008).
51. N. K. Tyagi, W. A. Fenton, A. L. Horwich, GroEL/GroES cycling: ATP binds to an open ring before substrate protein favoring protein binding and production of the native state. *Proc. Natl. Acad. Sci. U.S.A.* **106**, 20264–20269 (2009).
52. R. L. Koder, J. L. R. Anderson, L. A. Solomon, K. S. Reddy, C. C. Moser, P. L. Dutton, Design and engineering of an O_2 transport protein. *Nature* **458**, 305–309 (2009).
53. K. Miyazaki, MEGAWHOP cloning: A method of creating random mutagenesis libraries via megaprimer PCR of whole plasmids. *Methods Enzymol.* **498**, 399–406 (2011).
54. K. Miyazaki, Creating random mutagenesis libraries by megaprimer PCR of whole plasmid (MEGAWHOP). *Methods Mol. Biol.* **231**, 23–28 (2003).
55. E. Quaite-Randall, A. Joachimiak, Purification of GroEL from an overproducing *E. coli* strain. *Methods Mol. Biol.* **140**, 29–39 (2000).
56. J. Martin, Assembly and disassembly of GroEL and GroES complexes. *Methods Mol. Biol.* **140**, 65–70 (2000).
57. J. Ybarra, P. M. Horowitz, Inactive GroEL monomers can be isolated and reassembled to functional tetradecamers that contain few bound peptides. *J. Biol. Chem.* **270**, 22962–22967 (1995).
58. S. Cheley, M. S. Malghani, L. Song, M. Hobaugh, J. E. Gouaux, J. Yang, H. Bayley, Spontaneous oligomerization of a staphylococcal α-hemolysin conformationally constrained by removal of residues that form the transmembrane β-barrel. *Protein Eng.* **10**, 1433–1443 (1997).
59. D. Stoddart, L. Franceschini, A. Heron, H. Bayley, G. Maglia, DNA stretching and optimization of nucleobase recognition in enzymatic nanopore sequencing. *Nanotechnology* **26**, 084002 (2015).
60. M. Suzuki, T. Ueno, R. Iizuka, T. Miura, T. Zako, R. Akahori, T. Miyake, N. Shimamoto, M. Aoki, T. Tanii, I. Ohdomari, T. Funatsu, Effect of the C-terminal truncation on the functional cycle of chaperonin GroEL: Implication that the C-terminal region facilitates the transition from the folding-arrested to the folding-competent state. *J. Biol. Chem.* **283**, 23931–23939 (2008).
61. M. Hayer-Hartl, Assay of malate dehydrogenase. A substrate for the *E. coli* chaperonins GroEL and GroES. *Methods Mol. Biol.* **140**, 127–132 (2000).
62. H. Okuda, C. Sakuhana, R. Yamamoto, Y. Mizukami, R. Kawai, Y. Sumita, M. Koga, M. Shirai, K. Matsuda, The intermediate domain defines broad nucleotide selectivity for protein folding in *Chlamydophila* GroEL1. *J. Biol. Chem.* **283**, 9300–9307 (2008).
63. G. Maglia, A. J. Heron, D. Stoddart, D. Japrung, H. Bayley, Analysis of single nucleic acid molecules with protein nanopores. *Methods Enzymol.* **475**, 591–623 (2010).

Acknowledgments: We are grateful to the National Center for High-Performance Computing in Taiwan. **Funding:** We thank the European Research Council (European Commission's Seventh Framework Programme, project no. 260884) for funding. V.V.M. thanks the Research Foundation–Flanders for the doctoral fellowship. **Author contributions:** C.-W.H. and V.V.M. performed the research. K.-C.T. produced the αHL-GroES$_L$ structure. P.-J.D.T. and J.M. carried out the EM visualizations. G.M. designed and supervised the research and wrote the paper. **Competing interests:** The authors declare that they have no competing interests. **Data and materials availability:** All data needed to evaluate the conclusions in the paper are present in the paper and/or the Supplementary Materials. Additional data related to this paper may be requested from the authors. Raw data can be requested from C.-W.H. (chingwenho@pbf.com.tw) or G.M. (g.maglia@rug.nl).

Submitted 8 July 2015
Accepted 25 September 2015
Published 11 December 2015
10.1126/sciadv.1500905

Citation: C.-W. Ho, V. Van Meervelt, K.-C. Tsai, P.-J. De Temmerman, J. Mast, G. Maglia, Engineering a nanopore with co-chaperonin function. *Sci. Adv.* **1**, e1500905 (2015).